GUT MICROBES
2017, VOL. 8, NO. 6, 561–573
https://doi.org/10.1080/19490976.2017.1353843

Taylor & Francis
Taylor & Francis Group

RESEARCH PAPER/REPORT



# A bidirectional association between the gut microbiota and CNS disease in a biphasic murine model of multiple sclerosis

Sara L. Colpitts[a], Eli J. Kasper[a], Abigail Keever[b], Caleb Liljenberg[b], Trevor Kirby[b], Krisztian Magori[b], Lloyd H. Kasper[a], and Javier Ochoa-Repáraz[a,b]

[a]Department of Microbiology and Immunology, Geisel School of Medicine at Dartmouth College, Hanover, NH, USA; [b]Department of Biology, Eastern Washington University, Cheney, WA, USA

**ABSTRACT**

The gut microbiome plays an important role in the development of inflammatory disease as shown using experimental models of central nervous system (CNS) demyelination. Gut microbes influence the response of regulatory immune cell populations in the gut-associated lymphoid tissue (GALT), which drive protection in acute and chronic experimental autoimmune encephalomyelitis (EAE). Recent observations suggest that communication between the host and the gut microbiome is bidirectional. We hypothesized that the gut microbiota differs between the acute inflammatory and chronic progressive stages of a murine model of secondary-progressive multiple sclerosis (SP-MS). This non-obese diabetic (NOD) model of EAE develops a biphasic pattern of disease that more closely resembles the human condition when transitioning from relapsing-remitting (RR)-MS to SP-MS. We compared the gut microbiome of NOD mice with either mild or severe disease to that of non-immunized control mice. We found that the mice which developed a severe secondary form of EAE harbored a dysbiotic gut microbiome when compared with the healthy control mice. Furthermore, we evaluated whether treatment with a cocktail of broad-spectrum antibiotics would modify the outcome of the progressive stage of EAE in the NOD model. Our results indicated reduced mortality and clinical disease severity in mice treated with antibiotics compared with untreated mice. Our findings support the hypothesis that there are reciprocal effects between experimental CNS inflammatory demyelination and modification of the microbiome providing a foundation for the establishment of early therapeutic interventions targeting the gut microbiome that could potentially limit disease progression.

**ARTICLE HISTORY**
Received 3 October 2016
Revised 31 May 2017
Accepted 29 June 2017

**KEYWORDS**
dysbiosis; immunomodulation; gut-brain axis; gut microbiome; SP-EAE

## Introduction

Multiple sclerosis (MS) is a chronic autoimmune disease that affects the brain and spinal cord in the central nervous system (CNS). During MS, immune cells attack the myelin sheath that covers and protects neurons.[1] The resulting demyelination and eventual axonal loss ultimately leads to paralysis as myelin allows electric impulses to travel along the neurons. Distinct MS forms are described, but all cases cause devastating effects on the patient's health as well as provoking very significant social and economic consequences. The most common form of MS is relapsing-remitting MS (RR-MS) that affects 85% of the total patient population. RR-MS is initially diagnosed as a clinically isolated syndrome of neuronal dysfunction; a sequence of relapses and remissions follow over decades. CNS inflammatory processes drive these relapses causing the formation of pathological plaques in the white matter that characterize the disease. Approximately 70% of RR-MS patients develop secondary-progressive MS (SP-MS), mainly characterized by axonal loss and brain atrophy that causes a progressive neurologic impairment. During SP-MS the contribution of immune processes is reduced when compared with the relapses that characterize RR-MS.

Despite the large number of patients that suffer from SP-MS and the associated medical need, little is known about the cause(s) behind the transition from RR-MS to SP-MS. Multiple efforts are currently under exploration to obtain an efficient therapeutic against the progressive stages of the disease since most of the approved therapies against RR-MS are inefficient against SP-MS. Animal models that better resemble

**CONTACT** Javier Ochoa-Repáraz jochoareparaz@ewu.edu Department of Biology, Eastern Washington University, Cheney, WA 99004, USA.
Supplemental data for this article can be accessed on the publisher's website.

aspects of the pathology associated with chronic SP-MS are commonly used to understand the cellular processes involved in the transition to SP-MS. To study the process of demyelination and remyelination, the toxic cuprizone murine model is mostly used. Acute and chronic experimental autoimmune encephalomyelitis (EAE) experiments are largely performed using C57BL/6 and SJL mice or Lewis and Dark Agouti rats.[2] Alternatively, the non-obese diabetic (NOD) mouse model of EAE exhibits a biphasic pattern of disease progression that more closely resembles the human condition (RR-MS transitioning to SP-MS).[3-5]

Recent findings have revealed the importance of the intestinal microbiome in the development of CNS inflammatory disease. We have previously demonstrated that gut microbes[6] and symbiont factors[7-9] significantly influence gut regulatory immune cell populations and drive protection in the RR-EAE model. In this model, the onset of CNS disease promotes an increase in intestinal permeability that results from decreased expression of tight junction proteins within the intestinal epithelium.[10] Furthermore, significant changes in gut microbial abundances have been observed in MS patients compared with healthy individuals[11-13] and in a recent pediatric MS study.[14] These observations suggest that the communication between the host and the gut microbiota is bidirectional.

In this work, we propose that immunological changes that occur during different phases of disease modify the composition of the gut microbiome. We hypothesized that the gut microbiota relative abundances would differ between the acute inflammatory and chronic progressive stages of the NOD murine model of SP-MS. We also evaluated whether early and late alterations of the gut microbiota affected the progression of SP-EAE. Our results further suggest bidirectional communication along the gut-brain axis. Changes in the microbiome were relevant in the early stages of the disease. Our study also provided preliminary evidence suggesting that changes were characterized by reductions in certain genera, including the genus *Lactobacillus*, a gut bacterial component with demonstrated immunomodulatory effects in EAE.[15,16] Finally, we found that gut microbiome modulation early after disease induction significantly affected disease severity and progression. These observations provide support for a new therapeutic paradigm whereby the potential exists for reducing the progression to chronic stages of MS by targeting the gut microbiota soon following the establishment of relapsing-remitting disease.

## Results

### *Induction of EAE modifies the composition of the gut microbiota in NOD mice at early stages of disease*

We induced active EAE in 10 week-old female NOD mice as described previously.[3-5] EAE in NOD mice shows an incidence of disease of approximately 75%. In our study, 31 of 45 total EAE-induced mice (68.9%) exhibited disease progression, which is similar to what was described previously (Fig. 1A, Table 1). Mice initially developed a short phase of disease with reduced severity that subsequently progressed on to a severe form of EAE (*severe EAE* group). When averaging the clinical scores of the remaining 14 mice (31.1% of EAE-induced mice), the resulting pattern of EAE clinical scores showed a continuation of mild EAE disease throughout the duration of the experiment. Although one of the 14 mice developed a score of 2 (day 34), these mice did not progress into a severe form of EAE and, therefore, were grouped as '*mild EAE*' in the study (Fig. 1A, Table 1). EAE scores recorded for both mild and severe EAE groups showed an initial phase of disease that persisted from approximately day 9 through day 35 with scores averaging between 0.5 and 1. At day 35, the clinical disease scores for the severe EAE group progressed into greater disability of EAE with no apparent remissions, which was not observed in the mice grouped as mild EAE (Fig. 1A). A third group of control mice were not immunized with $MOG_{35-55}$/CFA and did not develop any spontaneous symptoms of EAE (no EAE group) (Fig. 1A). The area under the curve for the severe EAE mice was significantly elevated compared with the mild EAE mice; this difference also occurred between the severe EAE mice versus no EAE mice (Fig. 1B). In contrast, no significant differences were observed in the onset of disease between mild and severe EAE mice (Fig. 1C). Also, no significant differences were observed in the area under the curves for mild EAE mice vs. no EAE mice (Fig. 1B). The body weights of mice with EAE and controls were monitored weekly and no significant differences were observed when all EAE mice were grouped together (not shown). However, when the percentage of the initial weight was compared based

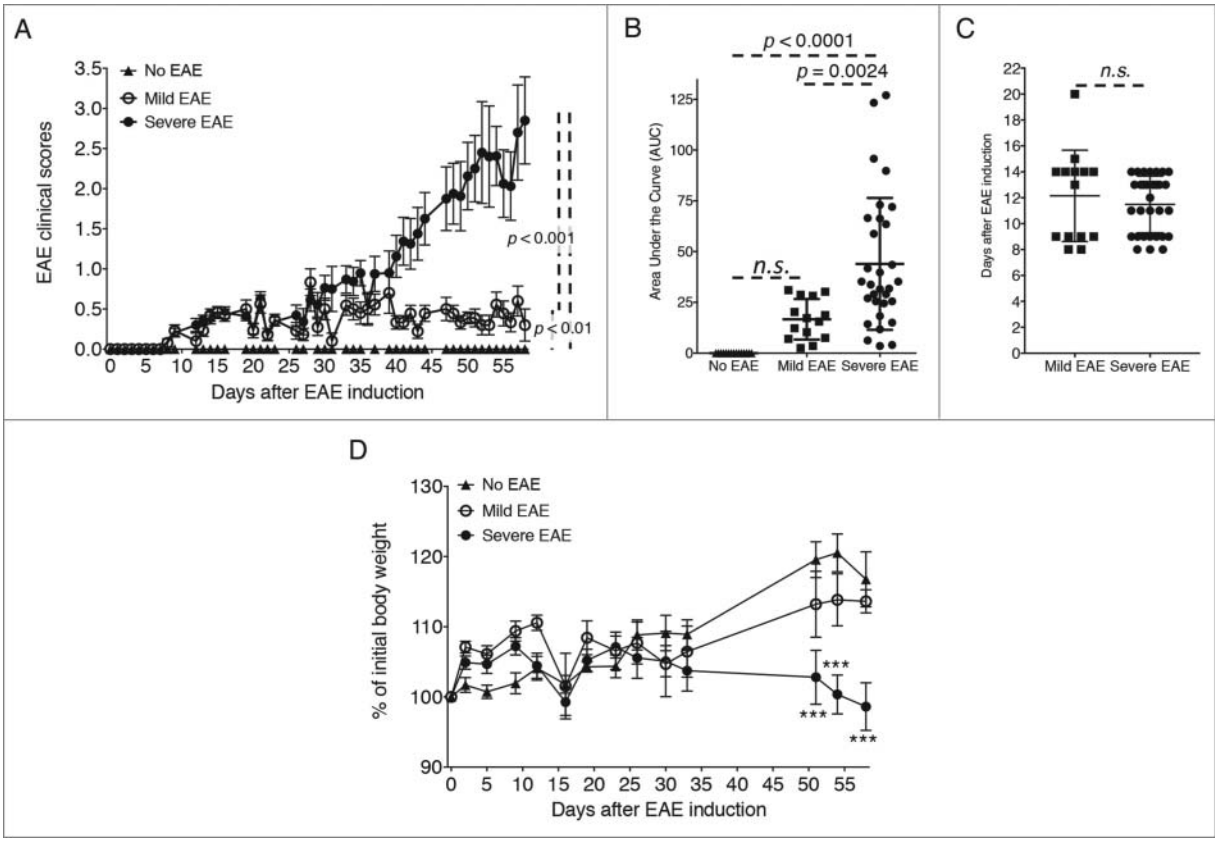


**Figure 1.** Active EAE induces a progressive CNS disease in mice. EAE was induced in NOD mice with a s.c. injection of $MOG_{35-55}$ emulsified in CFA and 2 doses of pertussis toxin (days 0 and 1) given i.p. Disease was induced in a total of 45 mice in 3 independent experiments. 25 NOD mice were used as controls (No EAE). (A) Graph depicts EAE clinical scores using a 0–5 scale from one of 3 experiments performed (No EAE n = 5; EAE-induced, n = 15). Scores were compared by one-way ANOVA followed by Tukey's multiple comparisons test (no EAE vs. mild, mild vs. severe EAE, and no EAE vs. severe EAE: $p < 0.001$). (B) Graphs indicate the area under the curve (AUC) of the clinical scores of all mice from the 3 experimental groups: no EAE n = 25, mild EAE n = 14 and severe EAE n = 31 mice. The AUCs were compared by one-way ANOVA followed by Tukey's multiple comparisons test. (C) Day of EAE onset for all mice from the 3 experimental groups, mild EAE n = 14 and severe EAE n = 31 mice, compared by students t- test. (D) Body weights of no EAE, mild EAE and severe EAE mice from one of the 3 experiments performed (no EAE n = 5, mild EAE n = 5, severe EAE n = 10). Percentages of body weights were compared by two-way ANOVA followed by Tukey's multiple comparisons test (No EAE vs. severe EAE: ***, $p < 0.001$).

on the form of disease that developed (mild vs. severe), we observed a significant decrease in weight gain in severe EAE vs. no EAE control mice (Fig. 1D).

To evaluate the effects of EAE induction on the composition of the gut microbiota at different stages of the disease, we grouped the mice to be analyzed at the end of the experiment when an overall assessment of disease severity could be established for individual mice (Fig. 1C). The samples were compared longitudinally from control mice without EAE (no EAE), mice that developed a mild form of the disease (scores 0.5 or 1; mild EAE), and mice that developed disease that corresponded with EAE scores equal to or above 1.5 for at least 2 consecutive days (severe EAE). Stool samples were collected at the day of EAE induction (day 0), day 14, day 30 and day 58. The clinical scores at the times of the collection are shown in Figure 2A. In total, stool

**Table 1.** Number of mice used, number and percentage of mice that developed mild and severe EAE, and day of disease onset.

| | Total/disease mice | % Disease | Day of onset (mean +/− SD) |
|---|---|---|---|
| EAE (45 mice) | | | 11.8 +/− 0.6 |
| Mild | 14 | 31.1 | 12.1 +/− 0.9 |
| Severe | 31 | 68.9 | 11.5 +/− 0.8 |
| No EAE (25 mice) | 0 | 0.0 | NA |

samples were isolated and compared from 15 out of the 70 mice used (Fig. 1 and described in Table 1). Mice within each group were never housed with mice from other groups. An analysis of the gut microbiota was performed by amplicon 16S rRNA (rRNA) gene sequencing to evaluate the relative abundances of the taxonomic groups and the total numbers of taxonomical levels: phylum, class, order, family, genus, and species. To determine whether the stage of disease affected the composition of the microbiome, we compared the level of similarity in the relative abundances of each taxonomic level identified at different time points throughout the course of EAE disease. To ascertain the effects of the genetic background of the stool microbiota of each individual animal compared, we first analyzed all samples prior the initiation of the experiment (day 0). The analysis was performed at the genus level by ordination analysis using nonmetric dimensional scaling (NMDS) in 2 dimensions (Fig. 2B). We used the NMDS combination with the lowest stress, i.e. the result having the smallest difference between the original dissimilarity of samples and generated after the simplified combination of the original taxa levels. After NMDS analysis, we applied the ADONIS multivariate non-parametric ANOVA and ran the ADONIS analysis with 10,000 permutations to obtain a distribution of $p$ values per comparison. By using the NMDS method, we aimed to obtain the optimal combination of the original taxa levels that illustrated the composition of the microbial communities across samples. No significant differences were observed among individuals grouped as no EAE, mild and severe EAE at day 0 ($p = 0.895$) (Fig. 2 and Table 2). When groups were compared individually (No EAE vs. Mild, No EAE vs. Severe and Mild vs. Severe EAE), no significant differences were observed (Table 2).

The Shannon diversity index, indicative of richness and evenness of the microbial community structure, of the stool samples isolated from mild EAE mice on day 14 was elevated when compared with no EAE mice (Fig. 2C: $p = 0.0267$). Although also increased in severe EAE mice, the results did not show any significant differences. Interestingly, when comparing the observed taxa (species level) of severe EAE mice vs. no EAE mice, a significant reduction was observed at day 58, indicating a lower number of species identified in EAE mice at the end of the experiment (Fig. 2C; $p = 0.0234$).

We next compared the overall composition of the microbiome of the 3 different groups on days 14, 30 and 58 at the genus level by 2-dimensional NMDS (Fig. 3A and Table 2). We first compared the microbiome composition of the control group (no EAE) at day 0 vs. days 14, 30 and 58 and observed no significant differences (day 0 vs. 14: $p = 0.0961$; day 0 vs. 30: $p = 0.0960$, day 0 vs. 58: $p = 0.0961$). Similarly, no significant differences were observed among the composition of the microbiome on day 14 vs. 30 ($p = 0.0962$), day 14 vs. 58 ($p = 0.0962$) and day 30 vs. 58 ($p = 0.0959$) (graphs not shown). When comparing the taxa grouped at the genus level on day 14, we observed an overall significant difference between the composition of the gut microbiome of controls without EAE, mild and severe EAE on days 14 ($p = 0.0034$) and day 30 ($p = 0.0096$), but not on day 58 ($p = 0.1915$) (Fig. 3A and Table 2).

On day 14 after disease induction, the gut microbiome of EAE mice was significantly different from the gut microbiome of control mice; No EAE mice vs. mild EAE ($p = 0.0406$) and no EAE vs. severe EAE ($p = 0.0167$). Furthermore, by comparing mild vs. severe EAE mice we observed that the extent of the disease also significantly affected the structural composition of the intestinal microbiome ($p = 0.0327$; Table 2) (Fig. 3A).

On day 30 post-EAE induction, significant differences were observed between mice with mild vs. severe EAE ($p = 0.0407$) and between mice with mild EAE and controls ($p = 0.0168$) (Table 2). In contrast, no overall significant differences were observed in the composition of the gut microbiome between the 3 experimental groups on day 58 post-EAE induction (Fig. 3A). Similar NMDS analysis and statistical comparison was performed at the phylum, class, order and family level, but no significant differences were observed when comparing all taxonomic levels at once (not shown). Based on these results, we postulate that EAE disease does in fact alter the composition of the gut microbiome of NOD mice. Furthermore, retrospective comparison indicates that animals that ultimately developed a severe form of EAE showed more profound alterations in the composition of the gut microbiome at early stages of disease.

At the phylum level, no significant differences were found when the identified sequenced counts were compared among groups (Fig. S1 for individual mice, Fig. S2 for averages per group, and Table S1). We next

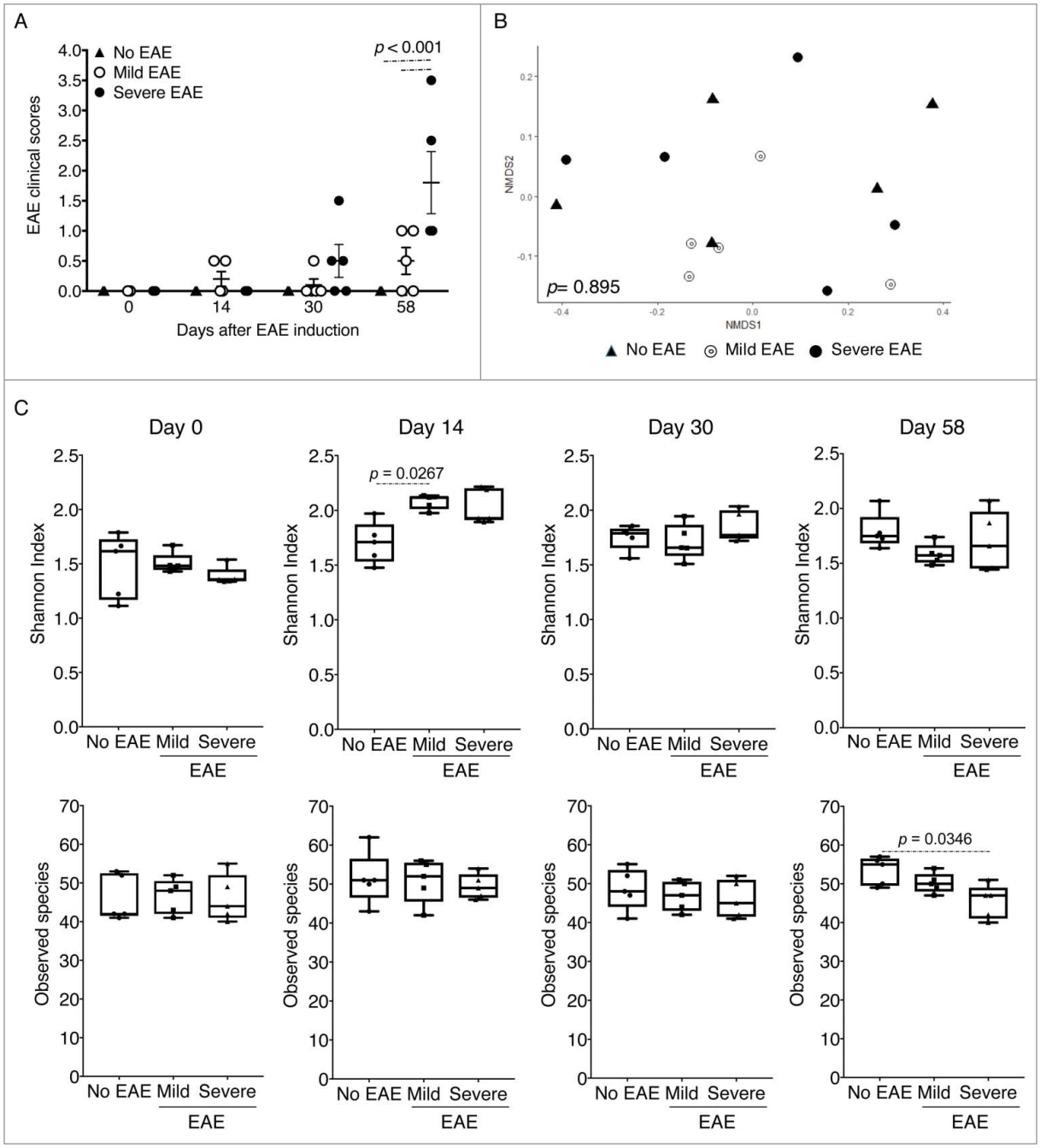


**Figure 2.** Composition of the microbiome at day 0, $\alpha$ diversity and species richness during disease. Stool samples were analyzed from No EAE control mice (n = 5), mice that developed mild disease (n = 5), and mice that developed severe EAE (n = 5). (A) Samples were collected from all 15 NOD mice. Clinical scores (mean +/− SEM) of mice at each time point of fecal collection (days 0, 14, 30 and 58 post-EAE induction) compared by two-way ANOVA. (B) To examine the compositional heterogeneity of the microbial communities found in the 3 groups, we used non-metric dimensional scaling (NMDS) in R to ordinate the microbial communities of samples based on the Bray-Curtis dissimilarity index using QIIME after the 16S rRNA (rRNA) gene sequencing analysis of stool samples, using the phyloseq package. Represented are the NMDS graph for the *genus* taxonomic level of OTUs identified in the analysis at day 0. The statistical comparison was performed using the permutational Multivariate Analysis of Variance Using Distance Matrices, ADONIS, in the vegan package. (C) Shannon index of $\alpha$ diversity and observed species measure in the 3 experimental groups compared by one-way ANOVA.

compared the effects of disease progression and severity on the relative abundances of members of genera among all major phyla. The relative abundances at the genus level are shown in Figure 3B (average relative abundances for $n = 5$ per group and timepoint) and Figure S6 (for individual samples per group and timepoint). The remaining taxonomic levels are represented in supplemental figures (Phylum: Figs. S1–2;

**Table 2.** Averages of the *p* values obtained after 10,000 different ADONIS analysis of the NMDS graphs for the genus level shown in Fig. 2 and 3A.

| | *Day 0* | *Day 14* | *Day 30* | *Day 58* |
|---|---|---|---|---|
| Overall | 0.8956 | 0.0034* | 0.0096* | 0.1915 |
| No EAE vs. Mild | 0.5000 | 0.0406* | 0.0168* | 0.1516 |
| No EAE vs. Severe | 0.9602 | 0.0167* | 0.3183 | 0.36548 |
| Mild vs. Severe | 0.8094 | 0.0327* | 0.0407* | 0.2230 |

*Note.* *, p <0.05 after ADONIS analysis repeated 10,000 times for each time point and comparison.

class: Fig. S3; Order: Fig. S4; Family: Fig. S5). Since the disease progression and severity impacted the overall microbiota structure (Fig. 3A and Table 2), we performed side-by-side comparisons among the sequence counts at the genus level among the 3 experimental groups (Tables S2–5, for day 0, 14, 30, and 58). A total of 39 out of the 158 genus level taxa showed raw *p* values below 0.05 when the 3 experimental groups were compared individually at any timepoint evaluated (Tables S2–5). However, the analysis showed no significant differences among genera when analyzing the adjusted *p* values obtained. We observed changes in the genus-level sequence counts of genera composition of the gut microbiota that resulted from the induction of disease, primarily noticed in the early stage of disease. An undetermined genus of the family *Ruminococcaceae* and the genus *Akkermansia* (Fam. *Verrucomicrobiaceae*) were increased in severe EAE mice vs. no EAE mice (Fig. S7). The genus *Turicibacter* was also increased in severe and mild EAE

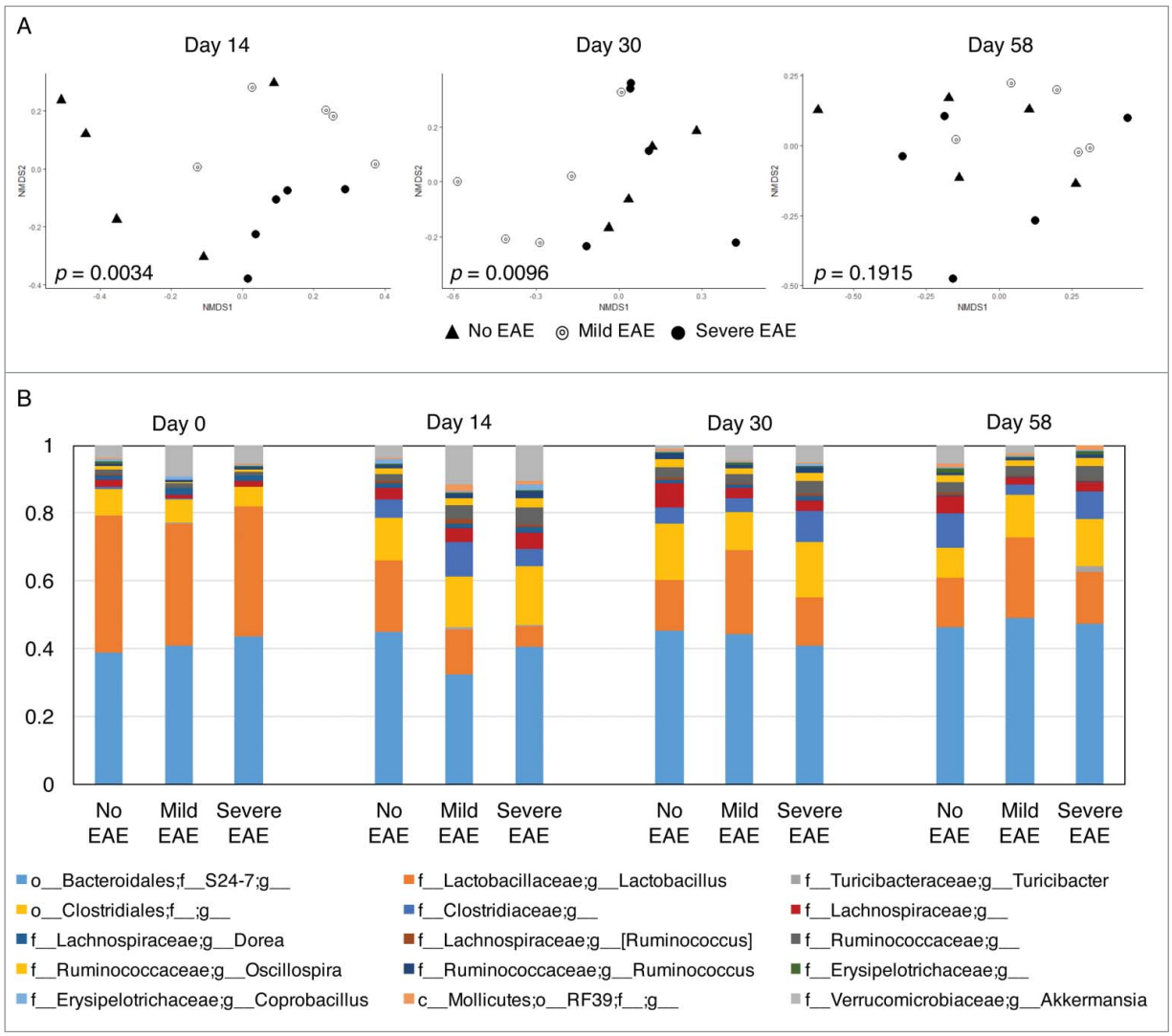


**Figure 3.** Early stages of EAE significantly affect the overall composition of the gut microbiome. (A) NMDS analysis for the *genus* taxonomic level of OTUs identified in the analysis at day 14, 30 and 58. (B) Relative abundances observed in analysis of the gut microbiota at the *genus* level. The bar graphs represent the average of relative frequencies per group (n = 5) per time point for abundances equal or above 1%.

when compared with controls, although at day 0 a raw $p = 0.008$ / adjusted: $p = 0.206$ was observed when comparing no EAE vs. mild EAE mice. The increased counts of undefined genus of *Ruminococcaceae* and genus *Akkermansia* in EAE mice were progressively reduced with disease. The numbers of *Akkermansia* were reduced in severe EAE mice to the point that at day 58 a raw $p = 0.008$ / adjusted: $p = 0.21$ was observed when compared with no EAE mice (Fig. S7).

The opposite pattern was observed for an undetermined genus of the family *Christensenellaceae* (Order *Clostridiales*) being increased in no EAE mice on day 14 (no EAE vs. mild EAE: raw $p = 0.008$ / adjusted $p = 0.17$; no EAE vs. severe EAE: raw $p = 0.008$ / adjusted $p = 0.22$) and day 30 (no EAE vs. mild EAE: raw $p = 0.008$ / adjusted $p = 0.20$; no EAE vs. severe EAE: raw $p = 0.008$ / adjusted $p = 0.21$). The increased counts of *Christensenellaceae* remained elevated on day 58 although no significant raw (and adjusted) $p$ values were detected. A similar pattern was observed in members of the genus *Lactobacillus* (fam. *Lactobacillaceae*, Order *Lactobacillales*). *Lactobacillus spp*. were reduced in mice with severe EAE when compared with control mice on day 14 (no EAE vs. severe EAE: raw $p = 0.008$ / adjusted $p = 0.17$) (Fig. S7).

Taken together, our results obtained from a retrospective analysis of stool samples from mice that were grouped based on the severity of their disease (mild vs. severe) suggested that mice that develop the most severe disease exhibit significant variations in gut bacterial genera at early stages of disease but that many of these variations are not long-lived and can continually change throughout the course of the disease (Fig. 3). Our findings, using an extended non-acute EAE model, indicate that different time points during the disease may differentially affect the gut microbiome. When comparing the individual genera, our findings show different patterns of change while disease progresses. However, our preliminary approach was unable to identify specific significant changes when adjusting the $p$ values to the total number of taxa observed.

### *Early alteration of the gut microbiota results in reduced disease progression and severity of EAE during the chronic stage*

We and others have previously documented the effects of the gut microbiota in regulating the progression of acute EAE when SJL and B6 mice were treated orally with broad spectrum antibiotics before the induction of disease.[6,17] Our work showed that treatment with antibiotics affected the balance of regulatory and proinflammatory responses in mice with EAE and that regulatory T cells (Tregs) were, at least in part, responsible for the protection achieved by modulation of the microbiota.[6] Similar observations were reported by Yokote and colleagues when altering the gut microbiota using a different combination of antibiotics,[17] but the authors proposed a protective mechanism dependent on invariant NKT cells. Studies in germ free mice have further confirmed the relevance of the microbiota in the establishment and progression of EAE disease.[18,19] In this current work, we evaluated whether oral antibiotic treatment would affect the progression of the secondary chronic stage of EAE in NOD mice. NOD mice were treated orally with neomycin, vancomycin, metronidazole, and ampicillin in the drinking water for 2 weeks (from day 0 of EAE induction to day 14). Control mice received normal drinking water. When comparing the course of the disease, the average clinical scores were significantly reduced in mice treated with antibiotics at multiple time-points after day 40 (Fig. 4A). An analysis of the area under the curves showed a significant reduction in the clinical disease scores of mice treated with antibiotics compared with untreated mice (Fig. 4B; $p = 0.0162$). Furthermore, treatment with antibiotics significantly delayed the onset of EAE (Fig. 4C; $p = 0.0005$) and reduced the overall severity index compared with untreated mice (Fig. 4D; $p = 0.008$). Because of the potential impact of antibiotic treatment on the overall health of the animals, we monitored the body weights in both groups weekly. At day 6 of the treatment, we observed a significant reduction in body weights of treated mice when compared with controls (Fig. 4E). However, the weights were restored by day 10, and overall no significant differences were observed by comparing the area under the curves (not shown; $p = 0.7295$). Flow cytometric analysis indicated that during EAE the frequency of $Foxp3^+$ Tregs increased in the Peyer's patches (Fig. 4F). We also observed similar increases in $CD39^+$ T cells and $Foxp3^+CD39^-$ Tregs.

We next compared the ability of oral antibiotics to reduce the severity of EAE disease when administered therapeutically after the onset of disease symptoms. This could only be accomplished using mice that

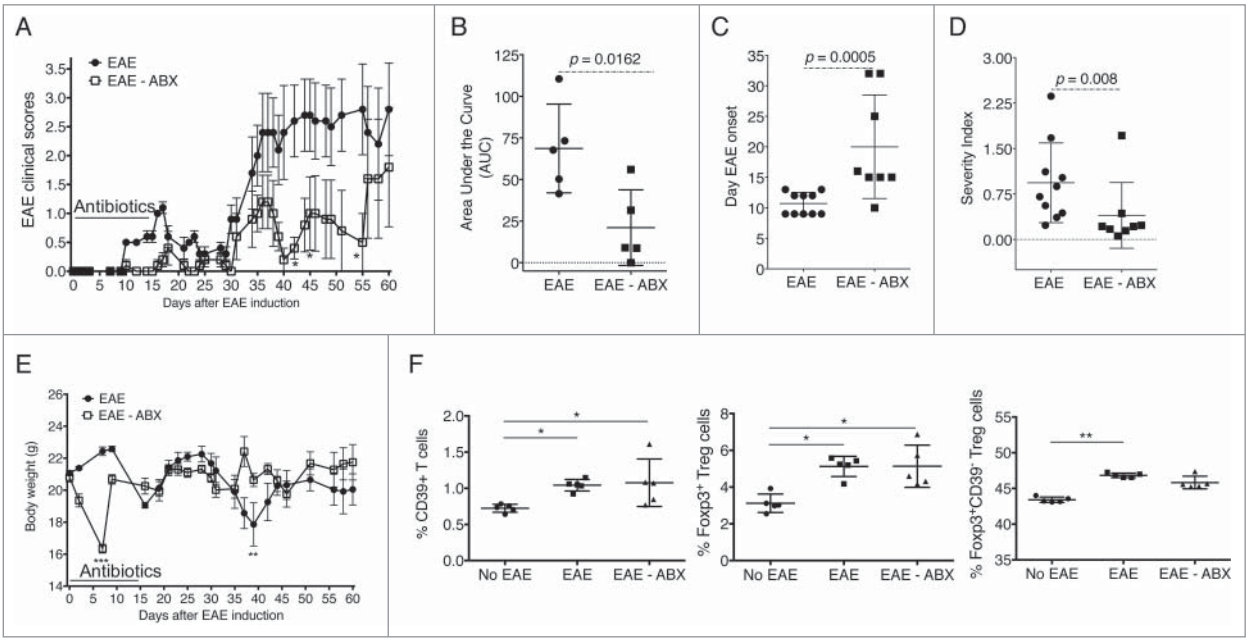


**Figure 4.** Early treatment with antibiotics reduces the severity of EAE in NOD mice. EAE was induced in NOD mice that were treated with antibiotics administered in the drinking water from days 0 to 14 or given normal drinking water as a control. (A) EAE clinical scores are shown from one of 2 independent experiments (n = 5), for a total of n = 8 per group. Two-way ANOVA followed by multiple comparisons test (*, $p < 0.05$). Graphs indicate the area under the curve (AUC) as calculated using Prism (B; n = 5 for the experiment depicted in panel A), the day of EAE onset (C), and the severity index [equals cumulative score divided by number of days with disease symptoms] (D). Panels C and D depict the values obtained for all mice combined between the 2 experiments (n = 8). Significance was measured using a Mann-Whitney test. E) Body weights are shown from one of 2 independent experiments for a total of n = 8 per group. Two-way ANOVA followed by multiple comparisons test (**, $p < 0.01$; ***, $p < 0.001$). (F) Graphs indicate frequencies of Tregs using flow cytometric analysis of live $CD4^+$ T cells in the Peyer's patches based on expression of Foxp3 and CD39 (n = 5 per group). Two-way ANOVA followed by multiple comparisons test (*, $p < 0.05$; **, $p < 0.001$).

survived the initial wave of CNS inflammation. Groups of mice were treated with antibiotics from day 30 to day 44 or day 69 to day 83 post-EAE induction. Control mice continued to receive normal drinking water. Overall, the mice that received antibiotics during the later stages of the disease showed a slight improvement in the clinical scores, however, no significant differences between antibiotic-treated and control groups were observed when all mice were pooled (Fig. S8). These findings suggest that early interventions targeting gut microbiota composition can affect the progression of disease in the long-lasting biphasic model of EAE in NOD mice.

## Discussion

During the last decade, evidence supporting the importance of the gut microbiota in human diseases has expanded exponentially. We and others have addressed the relevant regulatory effects that gut microbes, particularly bacteria, play in exacerbating or diminishing the severity of disease using a variety of experimental animal models of autoimmunity, including those that resemble MS. In this work, we explored the bidirectional nature of the gut-brain axis in the context of EAE, an inflammatory autoimmune disease of the CNS of mice. First, we questioned whether disease would affect the composition of the gut microbiota, and second, we addressed whether alteration of the gut microbiota would affect the progression of the disease using a biphasic murine model of EAE.

The NOD mouse model of EAE is characterized by an early stage of low grade disease severity followed by a more prolonged and exacerbated phase. Although it manifests a significantly longer disease model, its distinct stages allowed us to compare the composition of the microbiota at time points that correspond to varying degrees of clinical severity. Of note, as in human SP-MS, the reasons why this particular strain exhibits a biphasic disease pattern remain unknown. It was previously reported that a significant percentage of female NOD mice do not develop disease (approximately 25%).[3-5] In our study, we observed that 30% of mice used did not develop the expected severe

secondary phase of EAE. By contrast, these animals had a mild form of disease that was prolonged throughout the duration of the experiment, never transitioning to the severe stage. Long-term monitoring allowed us to retrospectively assign individual mice to one of the experimental groups before microbiome analysis. We compared the microbiota of those mice that developed severe secondary phase of EAE with those that developed mild EAE, in addition to control mice that were not induced with the disease (no EAE) (Fig. 1). Our results revealed that an altered gut microbiota was detected early following disease induction in mice that later developed EAE. The statistical analysis performed was unable to identify significant changes in specific genera associated with disease-induced dysbiosis. The lack of statistical significance based on adjusted $p$ values could be due to the reduced number of samples analyzed per time point. However, the results obtained with our preliminary study suggests that the disease progression and severity could impact the relative abundances of microbial populations associated with immunomodulation and disease regulation. The genus *Lactobacillus* and an undefined genus of the family *Christensenellaceae* were reduced (raw $p < 0.01$; adjusted: n.s) at days 14 and 30 of the experiment (Fig. S7). The immunomodulatory properties of members of the family *Lactobacillaceae* are already appreciated. A mixture of *Lactobacillus spp* has been shown to promote protection against murine EAE via the induction of IL-10-producing Tregs.[16] *Lactobacillus casei* strain Shirota (LcS) delayed the onset and reduced the severity of T1D in female NOD mice by restoring the Th1/Th2 balance.[20] Furthermore, VSL#3, a probiotic combination of *Bifidobacteriaceae* (*B. longum, B. infantis*, and *B. breve*), *Lactobacillaceae* (*L. acidophilus, L. paracasei, L. delbrueckii* subsp. *Bulgaricus*, and *L. plantarum*), and *Streptococcus thermophiles*, is protective against T1D through the induction of tolerogenic $CD103^{+}$ dendritic cells, a decrease in the effector T cell/Treg ratio, and a reduction in the population of intestinal Th1 and Th17 cells.[21] VSL#3 is also being extensively evaluated as a therapeutic against inflammatory bowel diseases[22] and MS.[23] *Christensenellaceae* are non-motile anaerobic Gram-negative, non-spore forming bacilli that belong to the order *Clostridiales*. Recent findings have shown that *Christensenellaceae* bacilli are highly hereditable among twins.[24] The implications of this work on our findings relate to the connection between the host genetic background and the heritability of the family *Christensenellaceae*. Since all mice used in our studies were obtained from the same inbred colony, we hypothesize that the reductions observed in *Christensenellaceae* during the course of EAE were caused by disease indicating that disease severity affects their relative abundance (Fig. S7). In other work, the levels of *Christensenellaceae* were reported as significantly enhanced in mice with lean body mass index (BMI) when compared with those showing obese BMI.[24] Recent evidence suggest that obesity and CNS diseases[25] might be connected through the effects of gut dysbiosis.[26]

By contrast, the results of our pilot study suggest a distinct pattern of taxonomical increases during EAE disease for members of the order *Clostridiales*, containing members of the family *Ruminococcaceae*, the family *Verrucomicrobiaceae (Akkermansia muciniphila* was identified) and the genus *Turicibacter* (Fig. S7). Little is known about the involvement of the family *Verrucomicrobiaceae* in autoimmunity. Increases in the abundances of *Turicibacteriales*, a *Firmicutes* family member that belongs to the class *Clostridiales*, have been reported in stool samples obtained from rheumatoid arthritis (RA) patients.[27] The relative abundances of other families of bacteria with known immunomodulatory effects, such as *Bacteroidaceae* were not affected (not shown). As mentioned above, a limitation of our study is the number of animals used in the analysis; however, the preliminary results suggest potential changes in the profile of bacterial genera that will require further and more profound attention.

In the second aim of our study, our results indicated that disease progression is significantly altered when mice receive oral treatment with antibiotics to alter the gut microbiota. Two weeks of treatment significantly delayed the onset of EAE disease (Fig. 4). Importantly, despite the long-term nature of the NOD-EAE model, the brief and temporary window of treatment significantly reduced the severity of the secondary phase of disease. We did not observe protection in mice treated with antibiotics after the onset of EAE symptoms (Fig. S8). Nevertheless, it is important to remark that by this stage of the disease the differences in the composition of the microbiota between groups were less pronounced. In addition, the secondary phase of EAE in the NOD model could be more neurodegenerative in nature including axonal loss,

astrogliosis, and microgliosis with reduced involvement of the immune system. Thus, the opportunity for improving disease by promoting immunosuppression may have already passed by the time we began antibiotic treatment. Future studies will address whether there is an association between disease progression, frequencies of certain bacterial populations, and the functional effects on the immunomodulatory cell populations in the gut.

In summary, in this initial study we showed using the NOD model of EAE that the composition of the gut microbiota is affected by disease progression. Furthermore, the positive effects of antibiotics at the onset of disease might suggest that appropriately timed antibiotic intervention to modulate the microbiota could be beneficial to limit the progression of CNS disease.

## Methods

### Mice and treatments

Ten-week old female NOD ShiLt (NOD/ShiLt) mice were obtained from the Jackson Laboratories. All animal care and procedures were in accordance with at Eastern Washington University institutional policies for animal health and well-being.

Mice subjected to oral antibiotic treatment were given drinking water with neomycin (1 g/L) (Fisher Bioreagents, BP2669–25), vancomycin (0.5 g/L) Fisher Bioreagents, BP2958–1), metronidazole (1 g/L) (Acros Organics, 210340050) and ampicillin (1 g/L) (Fisher Bioreagents, BP1760–25) for 2 weeks. Control mice received standard drinking water. Three different treatment windows were used depending on the experiment: 1) day 0 of EAE induction to day 14, 2) day 30 to day 44, or 3) day 69 to day 83. Body weights were measured on day 0 of EAE induction (at the initiation of treatment with antibiotics), every 3 d during antibiotic treatment, and weekly following the cessation of antibiotic treatment.

### EAE induction

EAE was induced with a Hooke Kit™ for EAE Induction (Hooke Laboratories, EK-2110) containing sufficient material per mouse for a single subcutaneous (s.c.) challenge with 200 $\mu$g $MOG_{35–55}$ emulsified in 200 $\mu$l of complete Freund's adjuvant (CFA). On days 0 and 1 post-challenge, mice received 400 ng of *Bordetella pertussis* toxin intraperitoneally (i.p.) (List Biological Laboratories, Campbell, CA; provided with Hooke Kit™ for EAE Induction). Mice were monitored and scored daily for disease progression as previously shown:[9] 0, clinically normal; 0.5, limp tip of tail (when picked up by base of tail, the tail has tension except for the tip); 1, limp tail; 1.5, limp tail and hind leg inhibition, slightly wobbly walking; 2, limp tail, hind leg weakness, wobbly walking, poor balance; 2.5, limp tail and hind legs dragging, poor balance; 3, limp tail, hind legs show complete paralysis, or limp tail with paralysis of one front leg and one hind leg; 3.5, limp tail, complete hind legs paralysis, and mouse moving but when placed on its side is unable to right itself; 4, limp tail, complete hind limb paralysis, partial front leg paralysis (mouse is minimally moving but appear to be alert and feeding); 5, mouse with minimal movement in front legs. No response to contact. Euthanized mouse due to severe paralysis. Per IACUC guidelines, mice were killed at scores of 3.5 and higher. The first of 2 concurrent days of scores of 0.5 or higher was documented as the onset of disease. NOD mice develop spontaneous type 1 diabetes (T1D) at week 14–20 of age[3] unless administered CFA, which prevents the induction of T1D,[28-30] and this approach is currently used to maintain NOD breeding colonies. We have performed multiple studies, including those described in this work. Among the approximate total of 120 mice used, only one mouse, at late stages of disease, showed clinical symptoms of T1D, with weight loss, excessive urination, and blood glucose levels above 300 mg/dL.

### Isolation of fecal samples and 16S rRNA (rRNA) sequencing

Stool samples were collected aseptically on days 0, 14, 30 and 58 and stored at −80°C. Samples were sent to AKESOgen (Norcross, GA) for 16S rRNA analysis of the microbiome. Qiagen DNA stool extraction kits were used for DNA isolation. One ng/ml of DNA aliquots were analyzed by PCR using primers specific to the variable region 4 (V4) of prokaryotic 16S rRNA gene. Library preparation and sequencing for V4 amplicon sequencing was performed on the Illumina MiSeq platform. Modified protocol with Nextera XT kit was used for library prep and sequenced using MiSeq V2(2 × 250bp) chemistry. AKESOgen used a protocol that combined the 2-steps in 1-step of amplification with forward primer(515F) and indexed-

reverse primer(806R). Once the sequencing was performed, we used a cloud-based web application for analyzing microbiome data from the Office of Cyber Infrastructure and Computational Biology (OCICB), National Institute of Allergy and Infectious Diseases (NIAID). Nephele. http://nephele.niaid.nih.gov/ (2016). QIIME was used for analysis[31] and R for statistical analysis. A total of 60 samples were compared using the QIIME FASTQ paired end protocol. Samples were pre-processed with a Phred quality score of 19 (99% base pair accuracy). Quality filters were applied to obtain a median sequence length of 253.0 per sample. 23435 total observations were found. The minimum and maximum number of counts obtained per sample were 174,345.0 and 573,715.0 respectively, with a mean +/− standard deviation of 287,059.183 +/− 75305.628. Reads that were demultiplexed were clustered into OTUs open reference approach by comparison with the Greengenes database allowing sequences clustered at 97% similarity. Analysis included the identification of chimeras (6,119 chimeras found) and removal using UCHIME. The OUT Table was rarified to 174,344 sequences per sample.

The abundance of each taxa were analyzed using the phyloseq package in R.[32] We visualized the compositional heterogeneity of the microbial community of each sample at every time point and at each taxonomic level using non-metric multidimensional scaling (NMDS[33]), the ordinate function in the phyloseq package and the metaMDS function in the vegan package,[34] and the Bray-Curtis dissimilarity index. We used 6 dimensions as it produced the lowest amount of stress, defined as the difference between the original dissimilarity and the dissimilarity based on a simplified combination of the original taxa.

Public access to raw sequences can be found at Sequence Read Archive (SRA) at NCBI (BioProject ID: PRJNA383155).

### Cell preparation and flow cytometry

Single cell lymphocyte preparations from Peyer's patches were stained using conventional methods. A live/dead fixable fluorescence-labeled viability dye (BD Biosciences, 564407) was used in all staining protocols, and samples were gated on viable cells for subsequent analysis. Cell subsets were analyzed using fluorochrome-conjugated mAbs against T cell antigens CD3 (BD PharMingen, 553062), CD4 (BD PharMingen, 553052), and CD39 (BioLegend, 143804). Intracellular staining for Foxp3 was performed using fluorochrome labeled anti-Foxp3 mAb (clone FJK-16s; eBioscience, 175773–82). Samples were acquired using a BD Accuri C6 (BD Biosciences, San Jose, CA). Data was analyzed with FloJo software (FloJO LLC, Ashland, OR).

### Statistical analysis

Parametric and non-parametric *t*-tests and one-way ANOVA followed by Kruskal-Wallis comparison of multiple groups was applied to show differences in flow cytometric analysis. Area under the curve analysis followed by one-way ANOVA and multiple comparison tests were applied to show differences in EAE scores of no EAE, mild EAE, and severe EAE mice. Two-way ANOVA followed by multiple comparisons test was used to compare the scores of EAE and EAE-ABX mice. In addition, AUC followed by Mann-Whitney test was used to compare scores of EAE and EAE-ABX mice. Weights were compared by two-way ANOVA followed by multiple comparisons test. To compare severity index, Mann-Whitney test was used. To compare the onset of disease Mann-Whitney test was used. $p$-values $< 0.05$, $< 0.01$, $< 0.001$ and $< 0.0001$ are indicated. Disease effects on the overall microbiota structure was visualized by plotting the results by NMDS in 2 dimensions. Plots were obtained using the R vegan package. After multiple iterations the one showing the lowest stress was used to generate visuals and for statistical permutational Multivariate Analysis of Variance Using Distance Matrices, ADONIS,[35] a permutational form of a multivariate analysis of variance (MANOVA). Since it is a permutational method, it produces a slightly different $p$-value each time. To obtain reliable $p$-values, we repeated the ADONIS method 10,000 times and reported the average of those $p$-values for each taxonomic level, time-point and comparison (Table 2). Genus-level counts were compared using the non-parametric Wilcoxon Rank-Sum test (when comparing 2 sample or matched samples) (Supplemental Tables 1–5, and supplemental figure 7). Differences were considered significant with a $p$-value $< 0.05$. The graphs and the statistical analysis were performed using Prism 7 (GraphPad Software Inc., San Diego, CA).

## Disclosure of potential conflicts of interest

No potential conflicts of interest were disclosed.

## Acknowledgments

We thank Dr. Satterwhite and EWU's vivarium staff for their support. We thank the flow cytometry core facility of the School of Pharmacy at Washington State University in Spokane, WA, and particularly Dr. Diana Browing for allowing us access to their flow cytometer. This study used the Nephele platform from the National Institute of Allergy and Infectious Diseases (NIAID) Office of Cyber Infrastructure and Computational Biology (OCICB) in Bethesda, MD.

## Funding

This work was supported by National MS Society (NMSS) (award #PP3423).

## Literature cited

[1] Dendrou CA, Fugger L, Friese MA. Immunopathology of multiple sclerosis. Nat Rev Immunol 2015; 15(9):545–58; PMID:26250739; https://doi.org/10.1038/nri3871

[2] Croxford AL, Kurschus FC, Waisman A. Mouse models for multiple sclerosis: historical facts and future implications. Biochim Biophys Acta 2011; 1812(2):177–83; https://doi.org/10.1016/j.bbadis.2010.06.010

[3] Basso AS, Frenkel D, Quintana FJ, Costa-Pinto FA, Petrovic-Stojkovic S, Puckett L, Monsonego A, Bar-Shir A, Engel Y, Gozin M, et al. Reversal of axonal loss and disability in a mouse model of progressive multiple sclerosis. J Clin Invest 2008; 118(4):1532–43; PMID:18340379; https://doi.org/10.1172/JCI33464

[4] Encinas JA, Wicker LS, Peterson LB, Mukasa A, Teuscher C, Sobel R, Weiner HL, Seidman CE, Seidman JG, Kuchroo VK. QTL influencing autoimmune diabetes and encephalomyelitis map to a 0.15-cM region containing Il2. Nat Genet 1999; 21(2):158–60; PMID:9988264; https://doi.org/10.1038/5941

[5] Levy H, Assaf Y, Frenkel D. Characterization of brain lesions in a mouse model of progressive multiple sclerosis. Exp Neurol 2010; 226(1):148–58; https://doi.org/10.1016/j.expneurol.2010.08.017

[6] Ochoa-Repáraz J, Mielcarz DW, Ditrio LE, Burroughs AR, Foureau DM, Haque-Begum S, Kasper LH. Role of Gut Commensal Microflora in the Development of Experimental Autoimmune Encephalomyelitis. J Immunol 2009; 183(10):6041–50; PMID:19841183; https://doi.org/10.4049/jimmunol.0900747

[7] Wang Y, Telesford KM, Ochoa-Reparaz J, Haque-Begum S, Christy M, Kasper EJ, Wang L, Wu Y, Robson SC, Kasper DL, et al. An intestinal commensal symbiosis factor controls neuroinflammation via TLR2-mediated CD39 signalling. Nat Commun 2014; 5:4432; PMID:25043484; https://doi.org/10.1038/ncomms5432

[8] Wang Y, Begum-Haque S, Telesford KM, Ochoa-Reparaz J, Christy M, Kasper EJ, Kasper DL, Robson SC, Kasper LH. A commensal bacterial product elicits and modulates migratory capacity of CD39(+) CD4 T regulatory subsets in the suppression of neuroinflammation. Gut Microbes 2014; 5(4):552–61; PMID:25006655; https://doi.org/10.4161/gmic.29797

[9] Ochoa-Repáraz J, Mielcarz DW, Wang Y, Begum-Haque S, Dasgupta S, Kasper DL, Kasper LH. A polysaccharide from the human commensal Bacteroides fragilis protects against CNS demyelinating disease. Mucosal Immunol 2010; 3(5):487–95; PMID:20531465; https://doi.org/10.1038/mi.2010.29

[10] Nouri M, Bredberg A, Weström B, Lavasani S. Intestinal barrier dysfunction develops at the onset of experimental autoimmune encephalomyelitis, and can be induced by adoptive transfer of auto-reactive T cells. PLoS One 2014; 9(9):e106335; PMID:25184418; https://doi.org/10.1371/journal.pone.0106335

[11] Jangi S, Gandhi R, Cox LM, Li N, Glehn von F, Yan R, Patel B, Mazzola MA, Liu S, Glanz BL, et al. Alterations of the human gut microbiome in multiple sclerosis. Nat Commun 2016; 7:12015; PMID:27352007; https://doi.org/10.1038/ncomms12015

[12] Chen J, Chia N, Kalari KR, Yao JZ, Novotna M, Soldan MMP, Luckey DH, Marietta EV, Jeraldo PR, Chen X, et al. Multiple sclerosis patients have a distinct gut microbiota compared to healthy controls. Sci Rep 2016; 6:28484; https://doi.org/10.1038/srep28484

[13] Miyake S, Kim S, Suda W, Oshima K, Nakamura M, Matsuoka T, Chihara N, Tomita A, Sato W, Kim S-W, et al. Dysbiosis in the Gut Microbiota of Patients with Multiple Sclerosis, with a Striking Depletion of Species Belonging to Clostridia XIVa and IV Clusters. PLoS One 2015; 10(9):e0137429; PMID:26367776; https://doi.org/10.1371/journal.pone.0137429

[14] Tremlett H, Fadrosh DW, Faruqi AA, Zhu F, Hart J, Roalstad S, Graves J, Lynch S, Waubant E, US Network of Pediatric MS Centers. Gut microbiota in early pediatric multiple sclerosis: a case-control study. Eur J Neurol 2016; 23(8):1308–21; PMID:27176462; https://doi.org/10.1111/ene.13026

[15] Maassen CB, van Holten JC, Balk F, Heijne den Bak-Glashouwer MJ, Leer R, Laman JD, Boersma WJ, Claassen E. Orally administered Lactobacillus strains differentially affect the direction and efficacy of the immune response. Vet Q 1998; 20 Suppl 3:S81–3; PMID:9689733; https://doi.org/10.1080/01652176.1998.9694976

[16] Lavasani S, Dzhambazov B, Nouri M, Fåk F, Buske S, Molin G, Thorlacius H, Alenfall J, Jeppsson B, Weström B. A Novel Probiotic Mixture Exerts a Therapeutic Effect on Experimental Autoimmune Encephalomyelitis Mediated by IL-10 Producing Regulatory T Cells. PLoS One 2010; 5(2):e9009; PMID:20126401; https://doi.org/10.1371/journal.pone.0009009

[17] Yokote H, Miyake S, Croxford JL, Oki S, Mizusawa H, Yamamura T. NKT cell-dependent amelioration of a mouse model of multiple sclerosis by altering gut flora. Am J Pathol 2008; 173(6):1714–23; PMID:18974295; https://doi.org/10.2353/ajpath.2008.080622

[18] Lee YK, Menezes JS, Umesaki Y, Mazmanian SK. Proinflammatory T-cell responses to gut microbiota promote experimental autoimmune encephalomyelitis. Proc Natl Acad Sci U S A 2011; 108 Suppl 1:4615–22; PMID:20660719; https://doi.org/10.1073/pnas.1000082107

[19] Berer K, Mues M, Koutrolos M, Rasbi ZA, Boziki M, Johner C, Wekerle H, Krishnamoorthy G. Commensal microbiota and myelin autoantigen cooperate to trigger autoimmune demyelination. Nature 2011; 479 (7374):538–41; https://doi.org/10.1038/nature10554

[20] Matsuzaki T, Takagi A, Ikemura H, Matsuguchi T, Yokokura T. Intestinal microflora: probiotics and autoimmunity. J Nutr 2007; 137:798S–802S; PMID:17311978

[21] Dolpady J, Sorini C, Di Pietro C, Cosorich I, Ferrarese R, Saita D, Clementi M, Canducci F, Falcone M. Oral Probiotic VSL#3 Prevents Autoimmune Diabetes by Modulating Microbiota and Promoting Indoleamine 2,3-Dioxygenase-Enriched Tolerogenic Intestinal Environment. J Diabetes Res 2016; 2016:7569431; PMID:26779542; https://doi.org/10.1155/2016/7569431

[22] Durchschein F, Petritsch W, Hammer HF. Diet therapy for inflammatory bowel diseases: The established and the new. World J Gastroenterol 2016; 22(7):2179–94; PMID:26900283; https://doi.org/10.3748/wjg.v22.i7.2179

[23] Tankou S, Bailey K, Regev K, Kivisäkk P, Ghandi R, Kirlis A, Cook S, Stuart F, Glanz B, Stankiewicz J, et al. Treatment of EAE and MS Subjects with Probiotic VSL#3. Neurology 2016; 86:P5.320.

[24] Goodrich JK, Waters JL, Poole AC, Sutter JL, Koren O, Blekhman R, Beaumont M, Van Treuren W, Knight R, Bell JT, et al. Human genetics shape the gut microbiome. Cell 2014; 159(4):789–99; https://doi.org/10.1016/j.cell.2014.09.053

[25] Ochoa-Reparaz J, Kasper LH. The Second Brain: Is the Gut Microbiota a Link Between Obesity and Central Nervous System Disorders? Curr Obes Rep 2016; 5(1):51–64; https://doi.org/10.1007/s13679-016-0191-1

[26] Ochoa-Repáraz J, Kasper LH. Gut microbiome and the risk factors in central nervous system autoimmunity. FEBS Lett 2014; 588(22):4214–22; https://doi.org/10.1016/j.febslet.2014.09.024

[27] Chen J, Wright K, Davis JM, Jeraldo P, Marietta EV, Murray J, Nelson H, Matteson EL, Taneja V. An expansion of rare lineage intestinal microbes characterizes rheumatoid arthritis. Genome Medicine 2016; 8:43; PMID:27102666; https://doi.org/10.1186/s13073-016-0299-7

[28] McInerney MF, Pek SB, Thomas DW. Prevention of insulitis and diabetes onset by treatment with complete Freund's adjuvant in NOD mice. Diabetes 1991; 40:715–25; PMID:2040388; https://doi.org/10.2337/diab.40.6.715

[29] Sadelain MW, Qin HY, Lauzon J, Singh B. Prevention of type I diabetes in NOD mice by adjuvant immunotherapy. Diabetes 1990; 39:583–9; PMID:2139617; https://doi.org/10.2337/diab.39.5.583

[30] Qin HY, Sadelain MW, Hitchon C, Lauzon J, Singh B. Complete Freund's adjuvant-induced T cells prevent the development and adoptive transfer of diabetes in nonobese diabetic mice. J Immunol 1993; 150:2072–80; PMID:8436836

[31] Caporaso JG, Kuczynski J, Stombaugh J, Bittinger K, Bushman FD, Costello EK, Fierer N, Peña AG, Goodrich JK, Gordon JI, et al. QIIME allows analysis of high-throughput community sequencing data. Nat Methods 2010; 7(5):335–6; PMID:20383131; https://doi.org/10.1038/nmeth.f.303

[32] McMurdie PJ, Holmes S. phyloseq: an R package for reproducible interactive analysis and graphics of microbiome census data. PLoS One 2013; 8(4):e61217; PMID:23630581; https://doi.org/10.1371/journal.pone.0061217

[33] Minchin PR. An evaluation of the relative robustness of techniques for ecological ordination. Minchin, P.R. Vegetatio 1987; 69:89–107; https://doi.org/10.1007/BF00038690

[34] Oksanen J, Blanchet F G, Kindt R, Legendre P, Minchin P R, O'Hara R B, Simpson G L, Solymos P, Stevens M H H, Wagner H. Vegan: Community Ecology Package. R package 2.2.1. http://www.worldagroforestry.org/publication/vegan-community-ecology-package-r-package-vegan-vers-22-1

[35] Anderson MJ. A new method for non-parametric multivariate analysis of variance. Austral Ecology 2001; 26:32–46.